Highlights of Spanish Astrophysics XII, Proceedings of the XVI Scientific Meeting of the Spanish Astronomical Society held on July 15 - 19, 2024, in Granada, Spain. M. Manteiga, F. González Galindo, A. Labiano Ortega, M. Martínez González, N. Rea, M. Romero Gómez, A. Ulla Miguel, G. Yepes, C. Rodríguez López, A. Gómez García and C. Dafonte (eds.), 2025

On the assembly state of dark matter haloes through cosmic history

Vallés-Pérez, D.[1], **Planelles, S.**[1,2], **and Quilis, V.**[1,2]

[1] Departament d'Astronomia i Astrofísica, Universitat de València, E-46100 Burjassot, València, Spain
[2] Observatori Astronòmic, Universitat de València, E-46980 Paterna, València, Spain

Abstract

The dynamical state and morphological features of galaxies and galaxy clusters, and their high-redshift precursors, are tightly connected with their assembly history, encoding crucial information about the formation and evolution of such cosmic structures. As a first step towards finding an optimal indicator of the assembly state of observed structures, we used a cosmological simulation of a moderate volume to critically examine the best definition of an indicator that is able to discriminate dark matter haloes undergoing mergers and/or strong accretion from haloes experimenting a relaxed evolution. Using a combination of centre offset, virial ratio, mean radial velocity, sparsity, ellipticity, and substructure fraction of the dark matter halo, we studied how the thresholds on these parameters, as well as their relative weights, should evolve with redshift to provide the best classification possible. This allows to split a sample of haloes in totally relaxed, marginally relaxed and unrelaxed subsamples. The resulting classification strongly correlates with the merging activity obtained from the analysis of complete merger trees extracted from whole simulation data.

1 Introduction

The *dynamical* or *assembly* state of galaxies, galaxy groups and clusters, and their underlying dark matter haloes, is a concept that has been frequently invoked in past literature, including both studies relating to the intracluster medium (ICM; [6, 11, 14]), or to their dark matter (DM) component [7].

However, there exist a plethora of different schemes for assessing it, including single parameters (e.g., virial ratio, centre offset; [3, 9]), categorical combinations of two parameters (e.g., [1]), as well as quantitative combinations of several of them [4]. Recent works have explored the space spanned by many proxies for dynamical state [5], suggesting that they can be split into roughly disjoint components representing different dimensions of dynamical state.

In this context, the *dynamical* or *assembly state* constitutes a rather loose concept, and it is important specifying under which particular properties is a halo being deemed as relaxed/unrelaxed. For the purpose of this work, we define the *assembly state* as the presence of recent mergers or periods of strong accretion (hence, a property drawn from the evolution of the halo). In turn, our *indicators* of dynamical state refer to properties of dark matter haloes (here, as inferred from the full, three-dimensional description obtained in simulations) at a given redshift (i.e., without making use of evolutionary information).

To the best of our knowledge, no work in the previous literature had considered a possible redshift evolution of their dynamical state classification schemes. In Vallés-Pérez et al. 2023 [13], we suggested a new way to combine a number of proxies for dynamical state through cosmic time, so that they best correlate with our notion of assembly state. While this is a short contribution, we refer the interested reader to the aforementioned work for a more in-depth description. These proceedings are organised as follows: in Sec. 2 we present our classification method and describe how it is calibrated. In Sec. 3 we show the classification parameters resulting from the calibration and some further tests. Finally, in Sec. 4 we draw the main conclusions from these results.

2 Methodology

We involve up to six indicators of dynamical state in this study, enumerated below. To avoid the additional uncertainties posed by baryons (especially in the central regions of clusters), all of them are computed using exclusively the DM distribution. Unless otherwise stated, they are computed within the virial radius, R_{vir}, of the halo, according to the prescription of Bryan & Norman [2].

- The centre offset, $|\vec{r}_{\mathrm{peak}} - \vec{r}_{\mathrm{CM}}|/R_{\mathrm{vir}}$, where $\vec{r}_{\mathrm{peak}}$ ($\vec{r}_{\mathrm{CM}}$) is the position of the density peak (centre of mass) of the halo.
- The virial ratio, $\eta = 2T/|U|$, where T and U are, respectively, the kinetic and gravitational potential energies of the halo.
- The mean radial velocity, $\langle v_r \rangle = \sum_\alpha m_\alpha v_{r,\alpha} / \sum_\alpha m_\alpha$, where $v_{r,\alpha}$ is the radial velocity of the α-th particle, as a measure of whether the halo is undergoing strong structural changes. We normalise this quantity by the circular velocity at the virial radius so as to obtain a dimensionless indicator, $\langle \widetilde{v_r} \rangle = \langle v_r \rangle / \sqrt{G M_{\mathrm{vir}} / R_{\mathrm{vir}}}$.
- The sparsity, $s_{200c,500c} = M_{200c}/M_{500c}$, where $M_{\Delta c}$ is the mass in a sphere enclosing a mean DM density Δ times the critical density of a ΛCDM universe.
- The ellipticity of the DM halo, $\epsilon = 1 - c/a$, where $a \geq b \geq c$ are the semiaxes of its mass distribution in non-increasing order.
- The fraction of mass in substructures, $f_{\mathrm{sub}} = M_{\mathrm{sub}}/M_{\mathrm{vir}}$.

Note that all six parameters should be positively correlated with the intuitive notion of unrelaxedness (i.e., in the path of a halo towards relaxation in the absence of relevant assembly episodes, the value of these parameters is expected to decrease). The classification scheme, given some thresholds, $\{X_i^{\rm thr}(z)\}$, on each parameter X_i and their corresponding weights, $\{w_i^{\rm thr}(z)\}$, will be so that:

- If $X_i < X_i^{\rm thr}(z)$ for all parameters i, the halo is classified as *totally relaxed*
- Else, the combination $\chi = \left[\sum_i w_i(z) \left(X_i / X_i^{\rm thr}(z)\right)^2\right]^{-1/2}$ is computed.
  - If $\chi \geq 1$, the halo is deemed as *marginally relaxed*.
  - Else, it is categorised as *unrelaxed*.

The calibration is performed by using the halo samples, extracted with ASOHF [12], of a $(100\,h^{-1}\,{\rm Mpc})^3$ volume simulation with peak resolution of $\Delta x \sim 10\,{\rm kpc}$ and $M_{\rm DM,finest} \sim 1.5 \times 10^7\,M_\odot$ performed with the adaptive-mesh refinement code MASCLET [8]. We determine the thresholds on these parameters by maximising, at each cosmic time, the similarity between the classification obtained from each individual indicator, and a fiducial classification based on the presence of mergers and periods of strong accretion in the last dynamical time. For more technical details on the calibration of the thresholds and weights, see Ref. [13].

3 Results

In Fig. 1, we present the main results on the calibration of the free parameters for the classification scheme, namely the thresholds (left-hand side panel) and the weights (right-hand side panel) on each dynamical state parameter, performed in the broad redshift interval $5 \geq z \geq 0$. For many of the parameters (most importantly, centre offset and sparsity), there is a strong redshift evolution on their thresholds, typically tending to increase towards higher redshifts. Meanwhile, for others (e.g., mean radial velocity), there is no significant evolution.

Interestingly, the weights on these parameters (which are proportional to the goodness of each indicator in splitting the merging and non-merging classes) also do undergo strong evolution. While at $z \simeq 0$ all indicators appear to perform similarly well and, hence, all weights are close to 1/6, the situation changes at higher redshifts. Towards $z \simeq 5$, some of the indicators (i.e., η, ε or $f_{\rm sub}$) become irrelevant in determining the assembly state of clusters, while others (Δ_r or $\langle \widetilde{v}_r \rangle$) dominate.

In Ref. [13], we tested our classification against a different simulation than the one used for the calibration, in order to assess its results. Using the `IllustrisTNG-DM CV-0` simulation from the CAMELS suite [15], in Fig. 2 we show, at $z = 0$, 1 and 2, the fraction of haloes in each of our assembly state classes which is actually undergoing mergers or strong accretion when tracking their evolutionary histories. As further discussed in Ref. [13] (cf. their Table 2), this classification outperforms all single parameters involved, as well as the most widely used combinations.

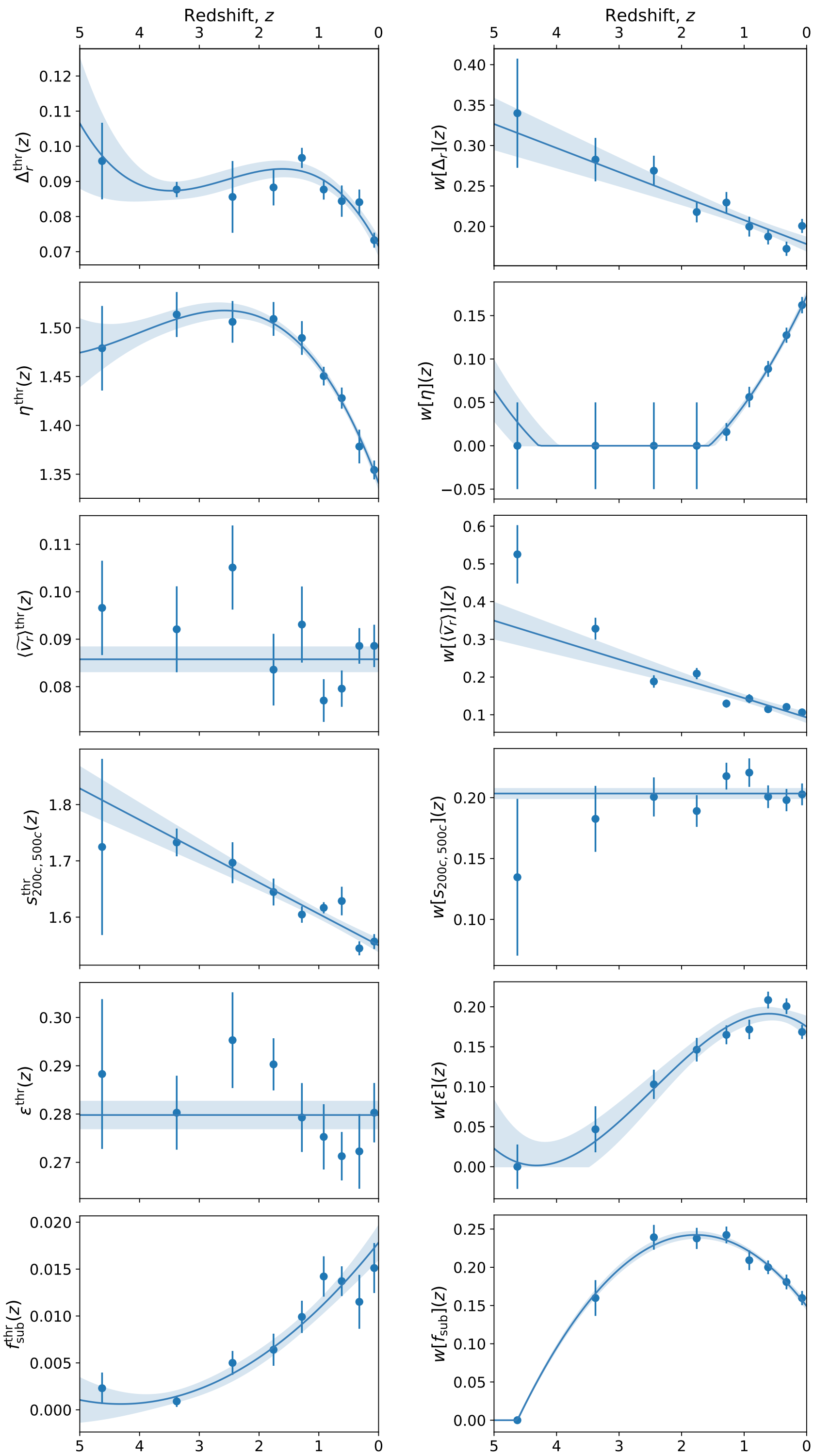

Figure 1: Calibration results on the thresholds on the dynamical state indicators (left) and their corresponding weights (right). In each panel, dots represent the estimations at each cosmic time, with the errorbars being standard errors computed from bootstrap resampling. Lines and their shaded regions are polynomial fits to this evolution with their respective confidence regions.

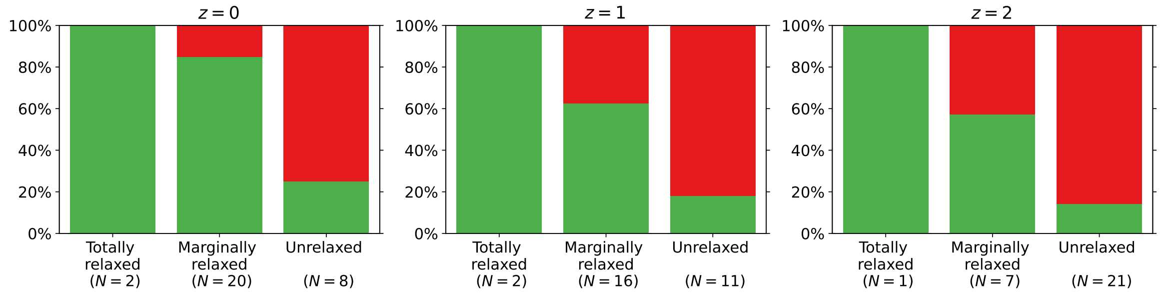

Figure 2: Classification assessment at $z = 0$, 1 and 2 (left, middle and right-hand side panels). Each column corresponds to a category of our classification. Within each bar, the green portion represents the fraction of haloes which have not suffered any mergers or strong accretion according to the fiducial classification. Reproduced from [13] with permission.

Finally, in Fig. 3 we exemplify, using the same data from the CAMELS suite, how our resulting classification has some predictive power on evolutionary quantities of the halo evolution, such as the time since the last merger (left-hand side panel), since the last major merger (central panel) or the accretion rates $\Gamma_{\rm vir}$ (right-hand side panel; [10]).

4 Conclusions

The results that we presented in this contribution suggest that the widely used schemes for the classification of the dynamical state of dark matter haloes or their baryonic counterparts (galaxies, groups and clusters) should not necessarily rely on fixed recipes (i.e., without redshift-dependence) if aimed at describing assembly state in its evolutionary sense.

The results provided here on how the different indicators depend on redshift, and their optimal combination to better match the true assembly history of haloes, could constitute relevant hints to find a suitable set of indicators applicable to observational data.

In the near future (Vallés-Pérez et al., submitted), we aim to show how these parameters and their combinations can provide quantitative information on the full assembly history of haloes, extending on the more categorical results shown in Fig. 3.

Acknowledgments

We thank the anonymous reviewer for their comments, which improved the presentation of these proceedings. This work has been supported by the Agencia Estatal de Investigación Española (AEI; grant PID2022-138855NB-C33), by the Ministerio de Ciencia e Innovación (MCIN) within the Plan de Recuperación, Transformación y Resiliencia del Gobierno de España through the project ASFAE/2022/001, with funding from European Union NextGenerationEU (PRTR-C17.I1), and by the Generalitat Valenciana (grant CIPROM/2022/49). DVP acknowledges support from Universitat de València through an Atracció de Talent fellowship. Simulations have been carried out using the supercomputer Lluís Vives at the Servei d'Informàtica of the Universitat de València.

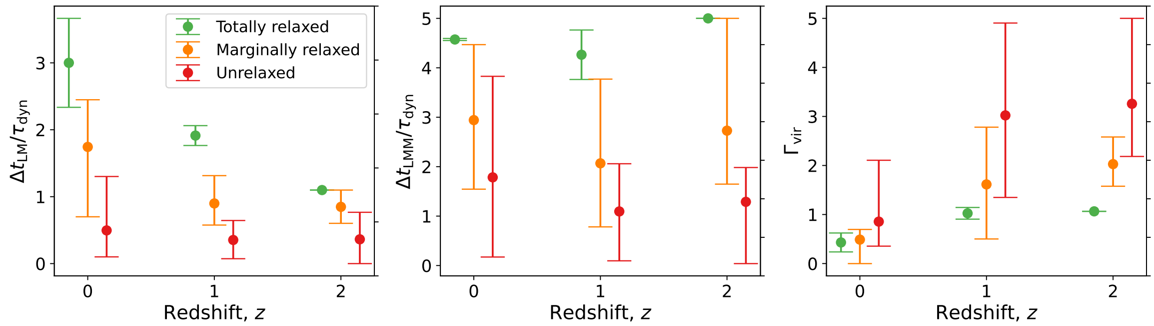

Figure 3: Evolutionary properties of the haloes according to their dynamical state classification. In each panel, red, orange, and green dots represent, respectively, the unrelaxed, marginally relaxed and unrelaxed subsamples. At each of the redshifts shown according to the x-axis, the dots and corresponding error bars (mean $\pm 1\sigma$) represent the time since the last merger (left-hand side panel) or major merger (middle panel) in units of dynamical times, and the accretion rates (right-hand side panel). Reproduced from [13] with permission.

References

[1] Biffi, V. et al. 2016, ApJ, 827, 112

[2] Bryan, G. L. & Norman, M. L. 1998, ApJ, 495, 80

[3] Crone, M. M., Evrard, A. E., Richstone, D. O. 1996, ApJ, 467, 489

[4] Haggar, R. et al. 2020, MNRAS, 492, 6074

[5] Haggar, R. et al. 2024, MNRAS, 532, 1031

[6] Lau, E., Nagai, D., Nelson, K. 2013, ApJ, 777 151

[7] More, S., Diemer, B., Kravtsov, A. V. 2015, ApJ, 810, 36

[8] Quilis, V. 2004, MNRAS, 352, 1426

[9] Shaw, L. D. et al. 2006, ApJ, 646, 815

[10] Vallés-Pérez, D., Planelles, S., Quilis, V., 2020, MNRAS, 499, 2303

[11] Vallés-Pérez, D., Planelles, S., Quilis, V. 2021, MNRAS, 504, 510

[12] Vallés-Pérez, D., Planelles, S., Quilis, V. 2022, A&A, 664, A42

[13] Vallés-Pérez, D. et al. 2023, MNRAS, 519, 6111

[14] Vazza, F. et al. 2013, MNRAS, 429, 799

[15] Villaescusa-Navarro, F. et al. 2021, ApJ, 915, 71